



Tropical Deep Convection, Cloud Feedbacks and Climate Sensitivity

Graeme L. Stephens^{1,2} · Kathleen A. Shiro³ · Maria Z. Hakuba¹ · Hanii Takahashi¹ · Juliet A. Pilewskie⁴ · Timothy Andrews⁵ · Claudia J. Stubenrauch^{6,7} · Longtao Wu¹

Received: 3 November 2023 / Accepted: 19 February 2024
© California Institute of Technology 2024

Abstract

This paper is concerned with how the diabatically-forced overturning circulations of the atmosphere, established by the deep convection within the tropical trough zone (TTZ), first introduced by Riehl and (Malkus) Simpson, in *Contr Atmos Phys* 52:287–305 (1979), fundamentally shape the distributions of tropical and subtropical cloudiness and the changes to cloudiness as Earth warms. The study first draws on an analysis of a range of observations to understand the connections between the energetics of the TTZ, convection and clouds. These observations reveal a tight coupling of the two main components of the diabatic heating, the cloud component of radiative heating, shaped mostly by high clouds formed by deep convection, and the latent heating associated with the precipitation. Interannual variability of the TTZ reveals a marked variation that connects the depth of the tropical troposphere, the depth of convection, the thickness of high clouds and the TOA radiative imbalance. The study examines connections between this convective zone and cloud changes further afield in the context of CMIP6 model experiments of climate warming. The warming realized in the CMIP6 SSP5-8.5 scenario multi-model experiments, for example, produces an enhanced Hadley circulation with increased heating in the zone of tropical deep convection and increased radiative cooling and subsidence in the subtropical regions. This impacts low cloud changes and in turn the model warming response through low cloud feedbacks. The pattern of warming produced by models, also influenced by convection in the tropical region, has a profound influence on the projected global warming.

Keywords Tropical convection · Cloud feedbacks · Climate change

Article Highlights

- The heating of the tropical trough zone drives circulations that affect remote cloud feedbacks and in turn global climate sensitivity
- The heating of the tropic zone is established by feedbacks between high cloud radiative heating and latent heating that are each by-products of convection
- Interannual variability of the high clouds in the tropics determines the interannual variability of the top-of-atmosphere (TOA) radiative imbalance of the tropics

Extended author information available on the last page of the article

1 Introduction

As the heated air of low latitudes rises and moves poleward, it cools and sinks in the subtropics creating a massive overturning of the atmosphere that stretches from the equator to the poles. This overturning circulation establishes both the main climate zones of Earth and the cloud patterns of these zones. That this rising, heated air at low latitudes is accomplished by the transports of many narrow plumes in deep convection, referred to as hot towers, was one of the most remarkable inferences about the atmosphere made in the mid-20th century by Riehl and Malkus (1958; hereafter R–M). Riehl and Simpson (1979; hereafter R–S) later revisited that study and estimated that about 1600–2400 hot towers must exist at any one time in the deep tropics under an assumption of a fixed size of 5 km.

Figure 1, adapted from Boucher et al. (2013), is a schematic depiction of the major cloud patterns of Earth and, more importantly, a schematic of their connection to the large-scale overturning circulations of the atmosphere. These connections begin with the area of deep convection at lower latitudes in the region referred to as the tropical trough zone (TTZ) by R–M. It is a zone where moisture is transported from higher latitudes at low levels and where heat is moved poleward in the upper levels. The TTZ is fundamental to the way that Earth’s heat engine moves heat from low latitudes to higher latitudes and establishes the latitudes where heat transport is toward the winter pole. Deep convection forms in this zone, and its seasonal changes are intimate parts of this transport which relates to the other major cloud types in ways hinted in Fig. 1. This includes high clouds that are directly produced by the convection and the low cloud regimes of the subtropics governed

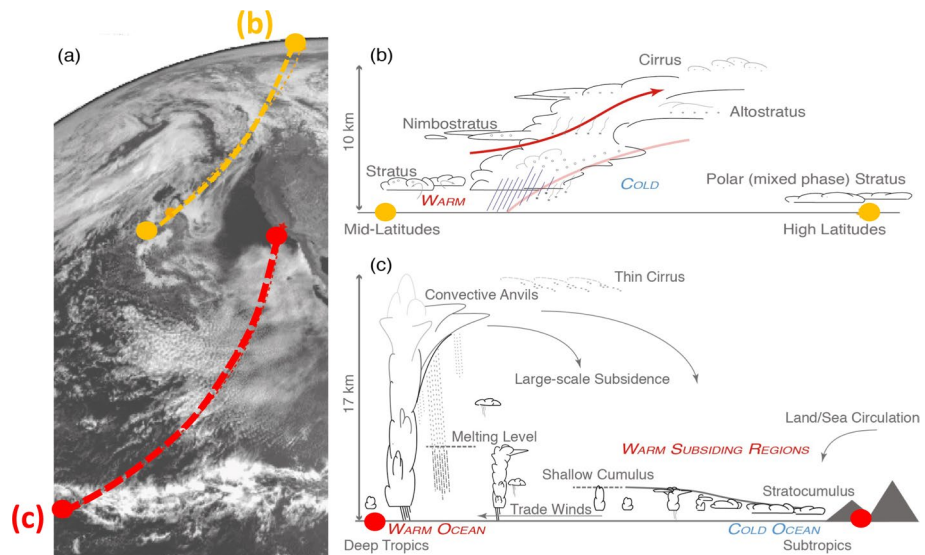


Fig. 1 **a** Visible imagery from geostationary satellite radiometer that shows clouds associated with extratropical cyclones, subtropical coastal stratocumulus near Baja California breaking up into shallow cumulus clouds in the central Pacific and mesoscale convective systems outlining the Pacific intertropical convergence zone (ITCZ) that resides in the tropical trough zone described later in the text. **b** A schematic section along the orange dashed lines highlighted in **a**, through a typical warm front of an extratropical cyclone. **c** A schematic section along the red dashed line in **a**, along the low-level trade wind flow from a subtropical west coast of a continent to the ITCZ [from Boucher et al. (2013)]

by the overturning circulation convection helps create. The influences of this circulation on clouds and, in turn, the influence of clouds on this circulation are a basic feedback cycle that frames all essential cloud feedbacks that regulate Earth's climate and its response to the forcing of climate change.

Some of the most important cloud feedbacks that are thought to operate on Earth can be traced to the circulations portrayed in Fig. 1 in a way that underscores how these feedbacks are indeed connected. This paper deals with only limited aspects of such connections, that of the influence of the deep convection that forms in the convergence zones of the tropics on cloud feedbacks that then occur both in these zones and further afield, all ultimately influencing Earth's global climate sensitivity, as expressed as the equilibrium climate sensitivity (ECS, Knutti et al. 2017). The paper first outlines data sources used to examine these influences. The initial focus of the paper begins in Sect. 3 with a review of the energy balance of the tropical convergence zone and radiative properties of clouds in that zone. Observations are used to frame our understanding about processes that are the bedrock of the cloud feedbacks widely discussed in the literature. Addressing these processes within the context of the current observed state and its variability, such as described in Sect. 4, and assessing model representations of these processes is an activity, although not specifically pursued in this paper in any detail, that is necessary to establish credibility in any model projection of change. Dessler (2010) is an example of how observations might offer some constraint or test of model feedback processes. Understanding gleaned from observed variabilities of Earth alone, while necessary, is an insufficient test of understanding as interactions of processes responsible for shorter-term observed variabilities do not always project onto longer term changes and do not always define how cloud feedbacks necessarily operate on this longer term. This is a point discussed more fully in later sections of the paper. Sections 5 and 6 expand the focus outward from the TTZ with an examination of the sensitivity of subtropical low cloud feedbacks on tropical convection and then on the sensitivity to deep convection of broader patterns of global warming and model estimates of ECS.

2 Sources of Data

A variety of different data types is examined throughout this study. These include:

- (i) The CERES Energy Balance and Filled (EBAF) Ed. 4.1 top-of-atmosphere (TOA) flux product (Loeb et al. 2018) with matching surface radiative flux data (Kato et al. 2018). These matched fluxes are made from a combination of observations and radiative transfer calculations archived in the form of monthly means for March 2000–March 2020 set on a $1^\circ \times 1^\circ$ latitude–longitude grid.
- (ii) Cloud properties consistent with the CERES EBAF flux product (Loeb et al. 2018) and matched in time are derived using the CERES-MODIS cloud retrieval algorithm (<https://ceres-tool.larc.nasa.gov/ord-tool/jsp/EBAF4Selection.jsp>). The cloud area fraction (CF) is the fraction of cloud identified in MODIS pixels within a CERES footprint based on the CERES-MODIS cloud mask algorithm and weighted by the total number of pixels within the footprint. The cloud effective pressure (we refer to it as cloud top pressure (CTP) although it does not necessarily denote the geometric top of the cloud) is derived from the cloud effective temperature (corresponding to the effective emission from clouds), which is based on the cloud's emissivity derived from the MODIS window channel temperature. The cloud visible optical

- depth (COD) is defined by the 0.65- μm channel radiances from cloudy pixels during daytime; during nighttime, COD is determined with the MODIS infrared channels, but this is limited to a narrow range of COD. We complement this cloud information with direct atmosphere opacity observations from CALIPSO (Guzman et al. 2017) to deduce temporal variability in tropical mean opaque cloud cover which are notionally clouds that attenuate the CALIPSO lidar approximately corresponding to COD > 3.
- (iii) The IMERG V06B monthly precipitation data are also used in the analysis, and these data are matched to the CERES gridded data at the same resolution of a 1×1 degree latitude-longitude (Huffman et al. 2020).
 - (iv) CloudSat radar data in the form of the 2B-Geopprof-lidar product (e.g., Mace et al. 2009). These data are used to characterize convective core intensity in this study based on past studies of Luo et al (2008) and Takahashi and Luo (2012). The deep convective core (DCC) is identified in the CloudSat profile data as profiles having (1) continuous radar echo from cloud top to within 2 km of the surface (i.e., the target cloud is rooted in the planetary boundary layer) and (2) echo top height (ETH) of the 10 dBZ reflectivity above 10 km. This core information is examined in more detail in related papers (Pilewskie et al. 2024; Derras-Chouk and Luo 2024).
 - (v) The multi-mission climate data record (CDR) of zonally averaged, monthly tropopause heights used here originates from the EUMETSAT Satellite Application Facility on Radio Occultation (RO) Meteorology (https://doi.org/10.15770/EUM_SAF_GRM_0001) and is derived from sounder measurements on Metop, COSMIC, GRACE and CHAMP. The dry temperature lapse-rate tropopause height is based on the standard WMO lapse-rate criterion which defines the tropopause at the lowest level at which (1) the lapse rate is less than 2 K km^{-1} and (2) the average lapse rate between this lower level and all levels within 2 km above it that does not exceed

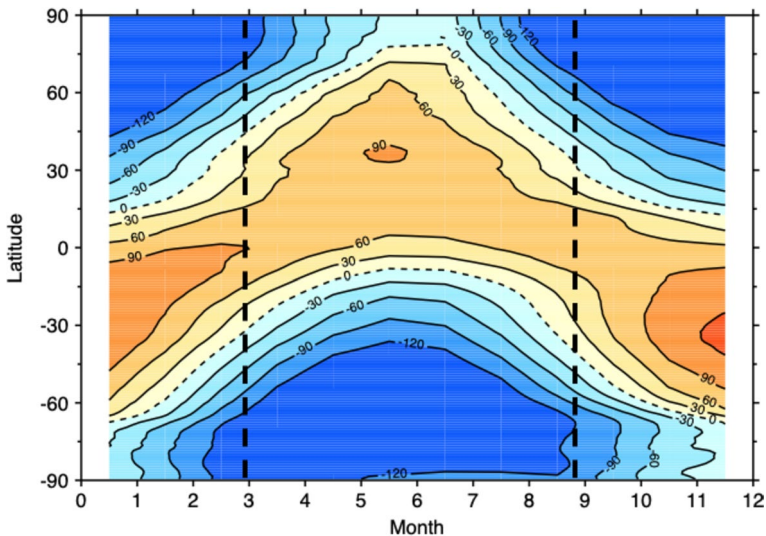


Fig. 2 The annual progression of the net radiation balance of the Earth-atmosphere system deduced from CERES radiative flux data (refer to discussion of data sources) where the fine dashed lines delineate the zero net flux. The vertical dashed lines identify times in the annual cycle used to define the extreme positions of the tropical trough zone. The contours of net flux are in Wm^{-2}

2 K km⁻¹. Further information on the data product can be found here: https://rom-saf.eumetsat.int/product_documents/romsaf_atbd_tph.pdf

- (vi) Radiative heating profile data of Stubenrauch et al. (2021) for the period 2004 to 2018. These radiative heating rate profiles have been extended in space and time from CloudSat FLXHR-lidar data (Henderson et al. 2013) by artificial neural network (ANN) regression models applied on cloud properties retrieved from AIRS (Stubenrauch et al. 2021) and atmospheric and surface properties from ECMWF re-analyses (Dee et al. 2011).

In addition to these observational data records, we also report on analysis of a number of CMIP6 experiments in Sects. 5 and 6. These analyses make use of data taken from CMIP6 model simulations (Eyring et al. 2016) from both the historical simulation experiment, from the amip-piForcing simulations, the abrupt-4xCO₂ simulations and the Shared Socio-Economic Pathway 5 (SSP5-8.5) simulations.

3 The Tropical Trough Zone (TTZ)

The seminal study of R–M provided the first estimates of the energy balance of the equatorial low-pressure trough zone in coordinates following the trough around the globe. Out of that study evolved the concept of convective hot towers and their fundamental role in the heat balance of this zone. Twenty years later, Riehl and Simpson (1979) revisited that study using updated global data available at that time, and noting some significant differences in the radiation balance between the two studies. Dramatic improvements in our ability to observe the global atmosphere and create globally consistent data records of the atmosphere have occurred since then with new satellite observations and re-analysis appearing at the apex of this improvement. Here, we provide a partial update only to these earlier studies applying the same analysis of R–S to define the seasonal location of this heated zone of the tropics with a brief description of the convection that forms within it. This latter aspect of the tropical trough zone is specifically discussed in more detail in a companion paper (Pilewskie et al. 2024).

As in R–S, the place to begin is the net radiation balance at the top of the Earth's atmosphere as shown in Fig. 2. This balance represents the entire column of the atmosphere, the Earth's surface and sub surface combined. If latitudinal energy transports are to be derived using these data on any basis other than annual, then the local heat storages of the atmosphere and oceans are needed. The atmospheric heat storage is small. Estimating the oceanic heat storage has been historically challenging, although ocean analyses approaches continue to improve (e.g., Forget et al. 2015) and could be considered as a source of heat storage information. Here, we adopt the simple approach introduced by R–M and compute the transports at those times when the ocean temperatures are at their maximum or minimum as these are times when local changes are near zero implying near zero ocean heat storage at these times depicted in Fig. 2 by the dashed vertical lines.

3.1 Meridional Energy Transports and the Positions of the TTZ

The meridional transports of energy corresponding to the times identified in Fig. 2 are presented in Fig. 3a. R–S argue that the transports derived at these times can be taken to be representative of longer periods and representative of transports to the respective summer and winter poles. When averaged together, as done in Fig. 3b, these transports should equal

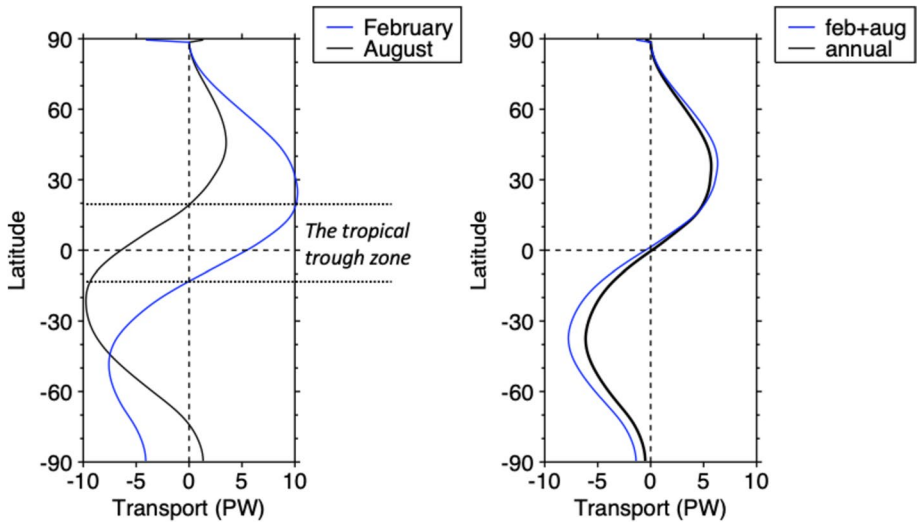


Fig. 3 **a** The atmospheric heat transports for February and August and **b** their combined transports compared to the annual total mean. The latter basically verifies the R–M approach/hypothesis that the February and August transports are largely atmospheric with their combination equivalent to the annual mean transport

that of the annual mean for the arguments of R–S to be valid. The small residual of this combined transport at the pole implies that a small amount of internal storage exists in the February analysis. Nevertheless, the close agreement between the summed transport and the annual mean transport revealed in Fig. 3b broadly supports the original arguments of R–S.

The dotted lines of Fig. 3a identify the latitudes that divide energy transports to summer and winter poles for both seasons. In combination, these define the position of the tropical trough for each season being the latitude of zero transport that is the latitude at which heat is moved in opposite directions to both poles. From analysis of these transports derived from the CERES radiative flux data, the tropical trough is determined to move annually between latitudes of 19 N and 13 S, which is a similar range to that originally identified in the R–S study although R–S subsequently argued for a more equatorial limit of the southern extent of this zone putting it at 5 S based on wind field analysis. We hereafter refer to this 19 N to 13 S region as the tropical trough zone (TTZ) and note a few important observations about it:

- (i) It is a fundamental zone containing deep convection, including the inter tropical convergence zone (ITCZ), and the net energy of it is always exported to the winter pole.
- (ii) The zone is asymmetrically positioned around the equator, being more weighted to the northern hemisphere (NH). This observation is consistent with our observation of the climatological annual mean position of the inter tropical convergence zones correspondingly lie in the NH, about which much has been written and is further discussed below (e.g., Philander et al 1996).
- (iii) This hemispheric asymmetry can be traced to the asymmetric heat losses of the respective NH and SH winter hemispheres. R–S note that it is the heating require-

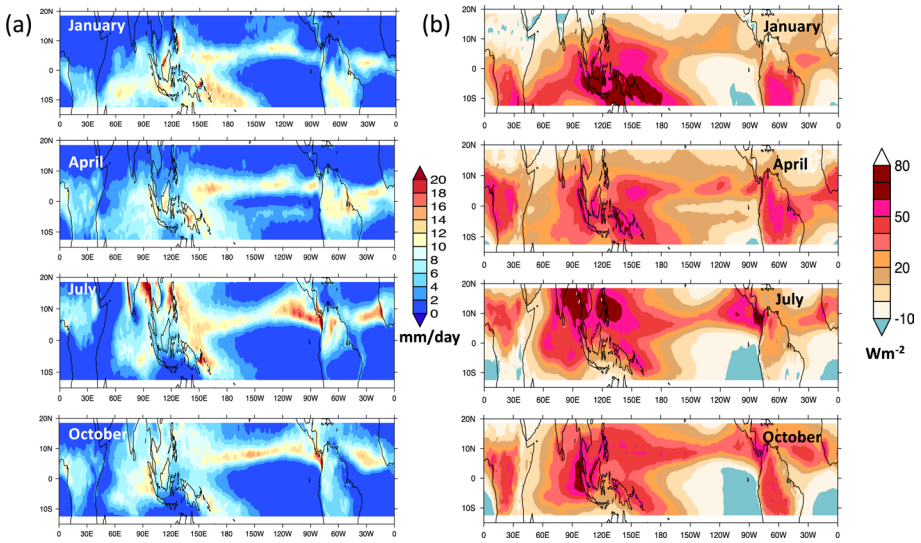


Fig. 4 **a** Left panels are January, April, July and October 22-year monthly mean distributions of IMERG precipitation within the TTZ and **b** right panels are the matching distributions of ACRE shown for comparison and discussed later in relation to Fig. 8

ment of the high latitude winter hemisphere that furnishes a constraint on the position of the trough and its range of displacement. A significant source of the greater heat loss from the SH winter hemisphere can be simply traced to differences in the amount of solar energy received by the respective winter hemispheres determined by differences in winter season Sun-Earth distance. This hemispheric asymmetry of the TTZ is consistent with our broad understanding of the displacement of the ITCZ favoring the warmer hemisphere (e.g., Broccoli et al. 2006). It is also consistent with studies that show a southward shift in convection as the energy transport northward increases to balance the increased loss of energy from the NH when increased cooling occurs at the higher NH latitudes (e.g., Kang et al. 2008, 2009; Frierson and Hwang 2012).

3.2 Convection in the TTZ

The variation of convection within the TTZ is often described as following the Sun. The pattern of change over the annual cycle is, however, more complex than this, being clearly shaped by different mechanisms of forcing that come into play. This point is well illustrated with reference to Fig. 4a which presents the 22-year mean IMERG precipitation climatology for 4 months. These months illustrate the shifting patterns of precipitation, and by inference convection, over the mean annual cycle. It is noteworthy that the largest total precipitation is not always aligned with the most intense convection, a point Zipser et al. (2006) noted and further elaborated on in the study of Pilweskie et al. (2023). The precipitation, and the convection that produces it, can be thought of in terms of three regimes governed by different forcing mechanisms. One is the regime of convection over the large southern land masses of S. America and the African continent. A second regime is that of

convection confined to narrow convergence zones more typical of the classical view of the ITCZ over the mid- and eastern Pacific and tropical Atlantic oceans, and a third regime encapsulates the convection of the maritime continent. The physical characteristics of convection within each of these regimes are further described in Pilweskie et al. (2023), while Derras-Chouk and Luo (2024) provide independent estimates of the mass transported vertically by the convection of these regimes. In a related paper, Roca et al. (2024) describe how the morphology of deep convection over Africa has changed over the 30 years of Meteosat observations shifting to smaller but longer-lived systems.

Convection over the tropical land masses indeed moves annually north and south following the movement of the Sun. This is evident in the shifting patterns of precipitation observed over these land masses and shown in Fig. 4a, being forced by surface heating that more-or-less tracks the Sun's position. According to Zipser et al. (2006), convection over these land masses is the most intense of all tropical convection according to TRMM radar data-based metrics of intensity, metrics that do not geographically align with maximum rainfall accumulations or other measures of convective activity, such as average IR cloud top temperature. The related studies of Pilweskie et al. (2013) and Derras-Chouk and Luo (2024), using different and more direct measures of convective intensity, including estimation of vertical motions, find convection over Africa to be the most intense of all deep convection on the planet.

The Maritime Continent, on the other hand, is an archipelago that includes Malaysia, Indonesia, the Philippines and Papua New Guinea and hundreds of islands of varying shapes and sizes. This complex geography, together with the fact it lies in some of the warmest waters on Earth, creates a complex set of interactions and circulations generated between ocean and land producing complicated precipitation patterns. The complexity of these patterns is exemplified in the pattern of the diurnal cycle of precipitation such as described by Wei et al. (2020). The maritime continent, also broadly referred to as the tropical western Pacific (TWP), is a major center for tropical atmospheric convection, and the latent heat released by the condensation of water vapor into cloud water and rain in this convection drives large-scale tropical circulations. Takahashi et al. (2023) offer a mechanistic explanation for why land-based deep convection is more intense than oceanic deep convection. The importance of the TWP to the global circulation is also reinforced in Derras-Chouk and Luo (2024) who find the TWP is a region of greatest mass fluxes of anywhere on the planet. As a consequence of this heating, and this mass flux produced by it, this region is a principal source of rising air in the tropics being the ascending branch of the Hadley and Walker circulations. As with convection over land, convection in the region of the maritime continent also undergoes a distinct seasonal cycle in a manner that also appears to follow the movement of the sun across the TTZ and is a key element of Earth's major monsoon systems.

The third regime is the convection that forms over the warmest waters of the Middle and Eastern Pacific and Atlantic oceans. Convection in this regime, unlike in the other regimes, does not follow the insolation maximum but sits north of the equator both in the Atlantic and Pacific being quasi-stationary throughout the year. Over the Pacific, convection remains largely anchored to the SST maxima that reside north of the equator that are more or less geographically fixed, according to Philander et al. (1996), by the asymmetry in positions of continents relative to the equator. The sea surface temperatures (SSTs) of the tropical Atlantic Ocean experience a small annual cycle with migration from the equator during the Boreal winter slightly northward of the equator during the Boreal summer (Crespo et al. 2019) with convection and precipitation following this migration.

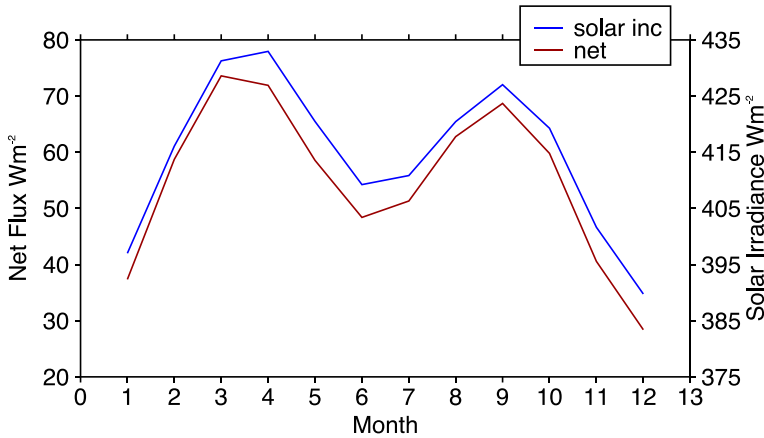


Fig. 5 The 22-year averaged annual cycles of TOA net radiation and daily mean solar irradiance of the TTZ

3.3 Radiative Properties of the TTZ

The radiative properties of the TTZ are now examined in the context of the convection that occurs in that zone. The connections between these properties and convection are elements of important cloud-convection climate feedbacks described later. All radiative properties reviewed here are derived from CERES EBAF data. In addition to the TOA net flux (Fig. 2), two sets of radiative flux properties are the focus of this section. First are the cloud radiative effects (CREs) defined at the TOA, and second are the atmospheric CREs (hereafter ACREs) representing the net absorption and emission by and from the atmosphere being the difference between the TOA and surface CREs. The monthly mean distributions of the ACRE are shown in Fig. 4b, and its comparison to the precipitation distributions of Fig. 4a and the implication of these comparisons are discussed below.

3.3.1 The Annual Cycle

The 20-year mean annual cycle of net radiative flux averaged over the TTZ is presented in Fig. 5 along with the annual cycle of the daily mean flux of incoming solar radiation. The annual cycle of net radiation, both in its phasing and amplitude, merely follows the incoming solar annual cycle that has a bimodal behavior established by the bimodal character of the daily mean TTZ averaged cosine of solar elevation. The tight correlation between the incoming solar and the net TOA flux ($R^2 = 0.98$) is a remarkable result in that all the factors that can be considered to affect the annual cycles of outgoing long and shortwave radiation, most notably cloud radiative effects discussed next, cancel although not entirely as discussed below. The extent of this cancelation is reflected both in the correlation between these two cycles and the rms flux difference between the two cycles which might be taken as an indicator of the degree to which internal processes influence the outgoing TOA fluxes on this time scale. This rms flux difference is 1.7 Wm^{-2} and, as we will see later in Sect. 4, is also of this same order as the interannual variations of net TOA flux forced by interannual changes in convection in the TTZ.

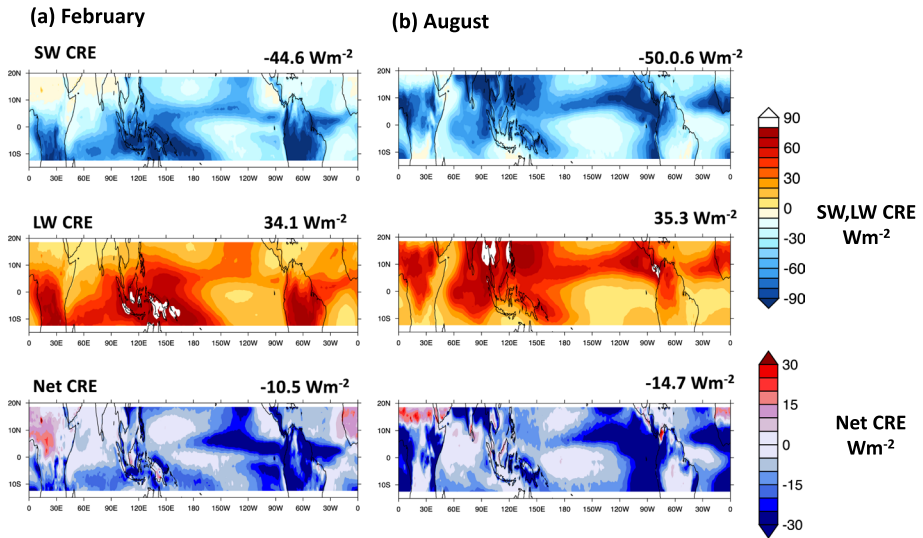


Fig. 6 a, b A 20-year climatology of the TTZ TOA cloud radiative effects for the 2 transition months (February and August) that define the latitudinal extent of the TTZ

3.3.2 Cloud Radiative Effects (CREs)

The discussion above notes a fact that has long been known—that the TOA longwave (LW) and shortwave (SW) components of outgoing radiation defined by clouds, and expressed as the net TOA CRE, cancel each other to a remarkable degree in lower latitudes. Figures 6 further illustrates this same point. Shown in Fig. 6, are the distributions of the SW and LW TOA CREs for the 2 months used to deduce the limits of the TTZ. Whether the regime where the CREs negatively mirror each other and cancel over the bulk of the TTZ that is purely coincidental or is part of an overall but as yet unknown constraint on the system still remains a mystery despite studies that have looked into the topic (e.g., Kiehl 1994). The degree to which this cancellation can be expected as Earth warms is also particularly pertinent (e.g., Sokul and Hartmann 2020) because small changes to one component without compensating changes to the other would constitute potential significant feedbacks (e.g., Stephens 2005). Existing tropical high cloud feedback concepts described in the next section are so posed, mostly hypothesized around changes to the LW component of the CREs or around the effects of high clouds on the ACRE.

While the majority of the climate change literature frames climate feedbacks almost exclusively in terms of changes to the TOA CREs, a number of studies over the years call out the importance of the in-atmospheric radiative heating by clouds not only for cloud-climate radiative feedbacks (e.g., Stephens et al. 2018; Needham and Randall 2021b) but also for feedbacks on global precipitation change (e.g., Stephens and Hu 2010). A number of studies have noted the influence of this heating on tropical convection and the ITCZ by, for example, its effect on the strength of the Hadley and Walker circulations (e.g., Slingo and Slingo 1988; Sherwood et al. 1994; Li et al. 2015; Harrop and Hartmann 2016; Popp and Silvers 2017). More recently Needham and Randall (2021b) argue that the ACRE of clouds associated with tropical convection is an important source of tropical heating that balances the horizontal export of energy out of the humid tropics by the large-scale

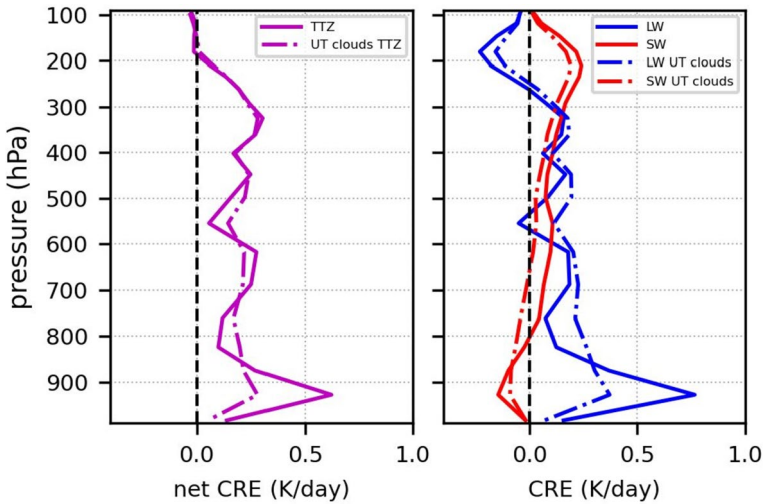


Fig. 7 The 2004–2018 averaged profiles of cloud radiative heating in the TTZ. The effect of all clouds (solid lines) is given by the radiative heating rate difference between all scenes and clear sky, while the effect of upper tropospheric clouds at a scale of 0.5° (broken lines) is given by the radiative heating rate difference between these clouds and those of clear sky, weighted by these clouds

overturning circulations. They recognized that this heating can be significant in inducing thermally direct circulations connecting humid and dry regions and further noted how the heating of the ACRE correlates to precipitation in the humid regions. The suggestion of a circulation driven in part by horizontal gradients of ACRE is not new and is a notion first suggested by Gray and Jacobsen (1977) and examined specifically by Slingo and Slingo (1988). Webster (1994) call it out as a mechanism central to the convection in the Western Pacific Warm Pool, and Stephens et al. (2008a) note its fundamental role in convective aggregation that occurs in numerical radiative convection equilibrium experiments. Before the CloudSat mission (e.g., Stephens et al. 2008b), however, the only way to estimate the ACRE was via model simulations of TOA and surface radiative fluxes. With the advent of cloud profile data, CloudSat observations provided the means to produce a more observationally-robust estimate of the global ACRE. These observations, along with others, were subsequently used to infer magnitudes of this differential heating associated with the warm phase of ENSO (Stephens et al. 2018).

The A-train data have also provided a mechanism for unambiguously defining the cloud structures responsible for the observed behavior of the ACRE as shown in Fig. 4b and explored further in discussion of Fig. 8. The effects of clouds and in particular of upper tropospheric clouds above 440 hPa on the radiative heating rates in the TTZ are presented in Fig. 7. The averages are given separately for the 24 h net CRE, LW CRE and 24 h SW CRE. The important point demonstrated by this figure is that it supports the assertions made above that it is the high clouds that most define the observed patterns of ACRE in the TTZ.

CloudSat measurements have also revealed how tropical cyclones that intensify versus weaker storms that do not contain greater amounts of ice in the high clouds in the vicinity of the storm center. This, in turn, is associated with larger ACRE and thus stronger radiative heating there. Similar to other studies mentioned above, Wu et al. (2023) show that an enhanced thermally direct circulation driven by a differential

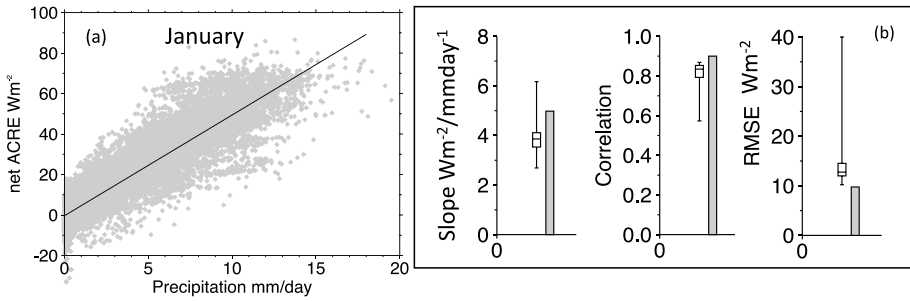


Fig. 8 **a** The correlation of monthly mean TTZ precipitation and the net ACRE. **b** The comparisons between the linear fit parameters of the data shown in **a** and the analogous fit to 26 the CMIP6 model produced data taken from the historical experiments. Model data are represented by the Box–Whisker diagrams

radiative heating formed between this enhanced heating in the vicinity of the center of the storm in contrast to the outer environment that further sustains the storm and is an important mechanism in cyclone intensification. They subsequently demonstrated that forecasts of intensity of tropical cyclones could be improved significantly when the forecast model better reproduces the observed spatial structure of this radiative heating.

An important point implicit to most of these past studies but often overlooked is how the radiative heating associated with high clouds in regions of convection reinforces the latent heating associated with the precipitation produced by the same convection thereby strengthening this thermally direct circulation. This is qualitatively evident in comparison of Fig. 4a, b noted previously and further reinforced with the scatter diagrams of Fig. 8. These scatter diagrams illustrate how the two main modes of diabatic heating of the TTZ atmosphere, in the form of the monthly mean diabatic ACRE and the monthly mean IMERG precipitation, are tightly coupled. The results shown in Fig. 8a apply to January only but are typical of the correlations observed for other months not shown. A linear-least-squares fit of the data is also provided for reference with a slope of $4.96 Wm^{-2}/mmday^{-1}$ and the prediction of net ACRE using precipitation as the predictor yields an ACRE rmse of $9.7 Wm^{-2}$. The same analysis was applied to the CMIP6 historical experiments for 26 models. These simulations span the period of extensive instrumental temperature measurements from 1850 to the present, and for the analysis performed only the model, January data for latter years of the simulations between 1995 and 2014 were used for comparison being nearer the period of the observational record. The comparisons are summarized in Fig. 8b in the form of box-quantile plots that define the maximum and minimum values of the 26 models, the 25th and 75th quantiles and the median compared to the observations of Fig. 8a that are summarized as a histogram bar. Except for one model outlier, all models produce similar high correlations between precipitation and the ACRE although the correlations of models are lower than that observed. On average, the model slope is also about 20% lower than the observed slope suggesting a weaker coupling between ACRE and precipitation in models than observed which hints at weaker couplings between convection (precipitation) and high clouds (ACRE).

4 The Interannual Variability of the Tropical Trough Zone (TTZ)

The feedback system involving the differential heating described above is also hypothesized to operate on interannual time scales (e.g., Stephens et al. 2018). Here the interannual variability of the energetics of the TTZ are further examined, with a focus of the total energy balance of the TTZ. Such variability hints at potential mechanisms of feedback associated with convection and the high clouds of the TTZ. As previously noted, almost all discussions of tropical high cloud feedbacks are framed around changes to the longwave component, that is the LW CRE, but the discussion above and the analysis now described also suggests that influences of high cloud changes on both the internal radiative heating of the atmosphere and on the TOA SW fluxes reflected to space cannot simply be overlooked. The importance of the latter is revealed in the data plotted in Fig. 9. The figure is a time series of a number of variables averaged over the TTZ all expressed as de-seasonalized anomalies. The time series of Fig. 9a illustrate the interannual variabilities of the TTZ-mean tropopause height (TROH) derived from COSMIC data contrasted against the anomalies of the CERES observed TOA energy imbalance (TEI). The time series of Fig. 9a reveals a distinct correlation ($R = -0.6$) between the interannual anomalies of the TTZ TROH and the corresponding changes to the TEI during the first half of the time series but with a lower correlation overall ($R = -0.36$) which is a reminder that different processes operate over the time period of the observations producing different responses in TEI. Figure 9b presents a measure of changes in convective intensity, similar in philosophy to that introduced by Zipser et al (2006), being a measure of the heights of the deep convective cores as defined by CloudSat observations (Takahashi and Luo 2012, 2014). This time series is limited by the availability of CloudSat observations. Figure 9c presents the matching time series of thick high clouds of the TTZ as defined by the opaque cloud product of CALIPSO (Guzman et al. 2017) again limited by data availability contrasted against the CERES net CRE.

The variabilities observed before 2017 presented in Fig. 9 in particular offer a consistent picture of the interannual variability of the TTZ. The depth of the TTZ troposphere undergoes a multi-year quasi-cyclic variation with periods of deepening and shallowing which have been connected both to ENSO and to the quasi—biennial oscillation and interannual variation of the Brewer Dobson Circulation (e.g., Davis et al. 2013; Li and Thompson 2013, Fueglistaler et al. 2009). The periods of deeper TTZ correspond to periods of deeper and more intense convection as suggested by a greater frequency of deep core convection observed by the CloudSat radar. Associated with this period of enhanced deeper convection is an increase of thick high cloud frequency which correlates to increased reflected sunlight from the TTZ during these periods. Further analysis of cloud property changes over the time frame of Fig. 9 is presented in Fig. 10 and supports the conclusion that the changes to the observed TEI that correlates to the TROH changes before 2017 are driven by changes to reflected sunlight from increasingly thick anvil clouds that form during times of deeper convection.

The spatiotemporal correlation analysis applied to monthly data for the period 2002–2022 identifies the cloud properties most responsible for the observed interannual variabilities and confirms the conclusion stated above. The properties examined include cloud fraction (CF), cloud top height/pressure (CTP) and cloud optical depth (COD). The anomalies of these three properties were normalized for comparison and correlated to the LW CRE, SW CRE and the net CRE anomalies. The results of this analysis as summarized in Fig. 10 lead to the following conclusion:

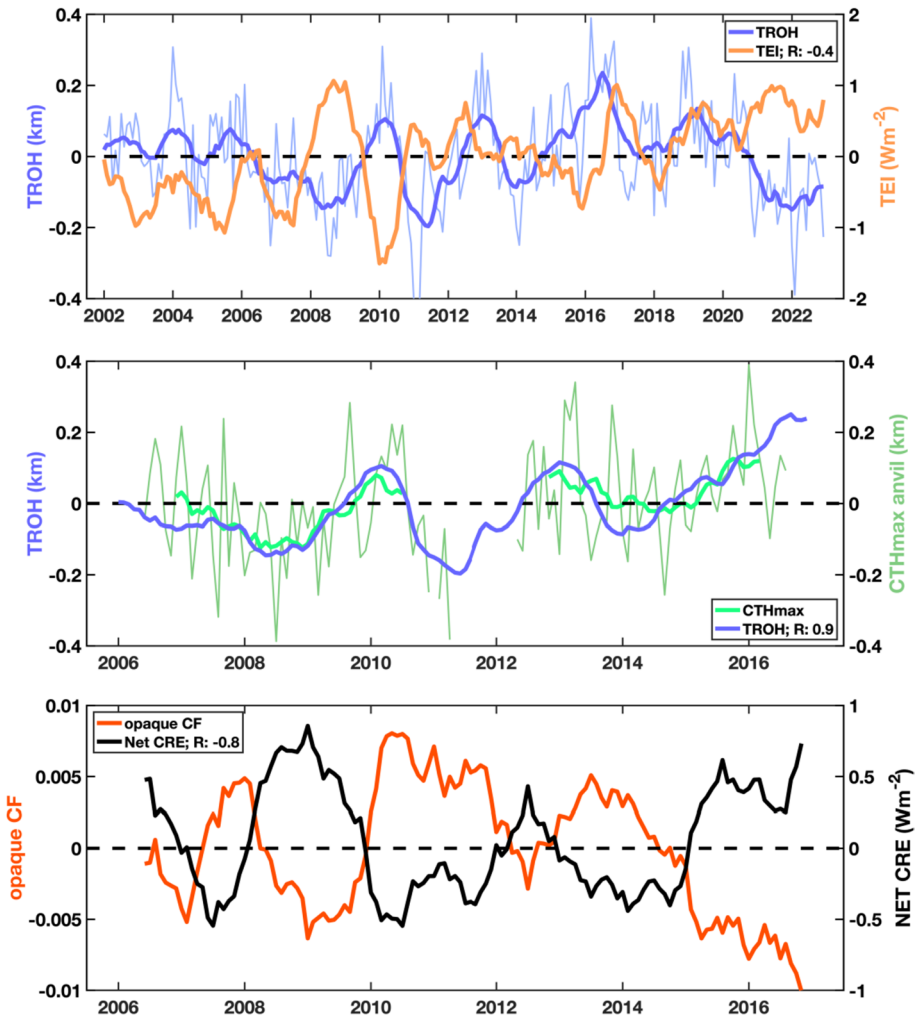


Fig. 9 **a** Time series of TROH (blue) and TEI (red) de-seasonalized monthly anomalies that are smoothed using a 5-month running mean filter, **b** time series of TROH (blue) and the convective cove maximum height (green) de-seasonalized monthly anomalies for a shorter time series than **a**. **c** Standardized monthly anomalies (unitless) smoothed with a 5-month running mean filter of tropical mean net CRE (black) and opaque cloud fraction (orange) with a correlation of -0.8 . The net CRE change is largely defined by the SW CRE (correlation of 0.7 , not shown), and the correlation SW CRE with COD (not shown) is -0.83 (Fig. 9f)

- (i) CF (Fig. 10 a, d, g) positively correlates ($R=0.75$) to the LW CRE and negatively correlates to the SW CRE ($R=0.7$) leaving a weak correlation overall ($R=-0.27$). This hints at the role of CF changes as a major factor in the LW-SW cancellation described above.
- (ii) An expected negative correlation exists between the LW CRE and CTP ($R=-0.75$; Fig. 10b) and a correlation of opposite sign exists between the SW CRE and CTP ($R=0.52$; Fig. 10e). A significant relationship between CF and CTP ($R=-0.7$)

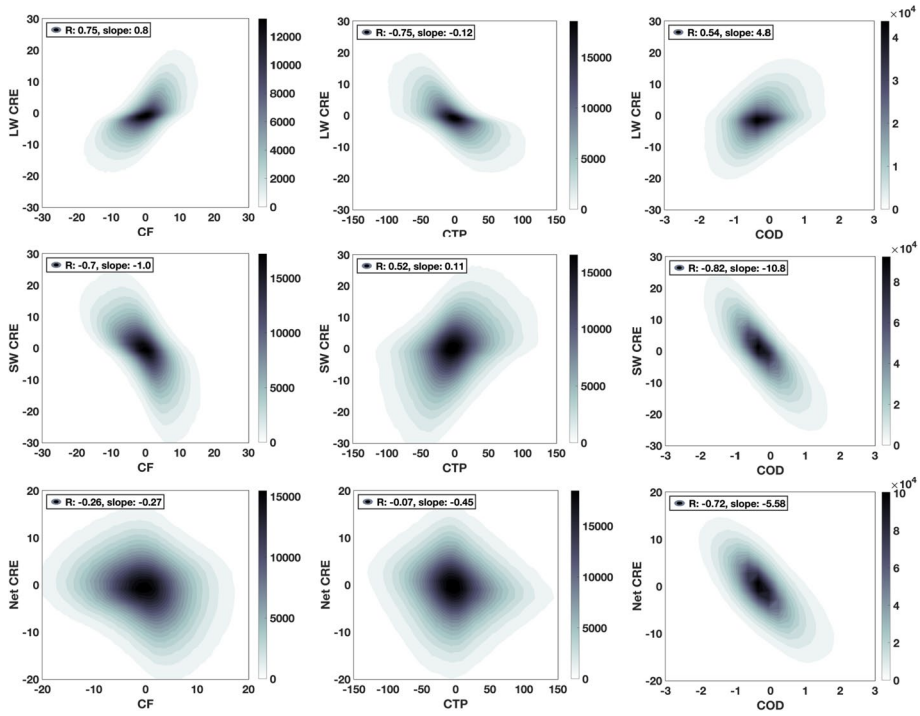


Fig. 10 Two-dimensional density scatter plots considering all space–time points in the TTZ over mid 2006 to end 2014 of cloud properties against radiative fluxes under cloudy conditions. **a** LWCRE versus cloud fraction (CF), **b** LWCRE versus cloud top pressure (CTP), **c** LWCRE versus cloud optical depth (COD), **d** SWCRE versus CF, **e** SWCRE versus CTP, **f** SWCRE versus COD, **g** Net CRE versus CF, **h** Net CRE versus CTP, and **j** Net CRE versus COD. Figure legends indicate the *R* correlations and regression slopes of the respective analyses. Shading indicates number density of data points

also exists (not shown) such that higher clouds are associated with enhanced CFs. The effect of CTP on the net CRE is nearly zero (Fig. 10h) with the spurious SW and LW responses to CTP again compensating one another. This strong correlation between CF and CTP implies that more intense convection (indicative of lower CTP) develop into larger convective systems (higher CF) as called out in number of previous publications have shown this relationship (e.g., Machado and Rossow (1993), Takahashi et al. (2017), among others).

- (iii) The most dominant cloud parameter of influence on the observed variability of the TEI for the period up to 2017 is the cloud optical depth (COD). The covariabilities of COD and CF ($R=0.4$) and COD and CTP ($R=-0.2$), respectively, are smaller than is the covariability of CF and CTP. While the LW CRE increases with COD, a result that suggests even the thinner, non-radiative black-body high clouds also thicken during periods of deeper convection, this response is much weaker than the overwhelming negative relationship between COD and the SW CRE ($R=-0.82$) that determines the net CRE response ($R=-0.72$). The strong correlation of the CALIPSO measure of thick high clouds with the timeseries of SW CRE ($R=-0.83$) and the net CRE ($R=-0.76$) further supports the conclusions that it is a thickening

of anvil clouds and increased SW reflection that determines the interannual variation of the spatially distributed TEI.

5 Cloud-Radiative-Convective Feedbacks in a Changing Climate

We consider now the influence of tropical convection within the context of climate change and do so with a focus on cloud feedbacks mostly relying on a number of climate model climate change experiments archived under CMIP6.

5.1 Tropical High Cloud Feedbacks

There is a growing literature on the topic of high cloud feedbacks that involve the interactions of convection, clouds and radiation. Some of that literature was described above in relation to the role of these clouds in heating the atmosphere. Other concepts exist that focus either on feedbacks at the surface or feedbacks involving the entire column as viewed through from the perspective of TOA CREs. Ramanathan and Collins (1991), for example, argued that the shielding of solar radiation by thick anvil clouds overwhelm the enhanced greenhouse effect that they induce in a moist, convectively active atmosphere over warm oceans, and suggested that these clouds act as a natural thermostat regulating the sea surface temperature (SST). Stephens et al. (2004) interpreted TOGA COARE observations as showing that the longwave radiative heating of the upper troposphere, induced by enhanced amounts of high clouds during active phases of the Madden-Julian oscillation (MJO), coupled with the solar radiation reduction at the ocean surface act together as a self-regulating radiative-convective system. A number of other ideas center on the longwave effect of anvil clouds. Lindzen et al. (2001) proposed an “iris” mechanism, built upon the assumption that precipitation formed in convection over warmer oceans will rain more efficiently with proportionally less water being transported aloft and detrained into anvil clouds. Anvil clouds produced by convection are then hypothesized to shrink in area as sea surface temperatures (SSTs) warm. The result is an increased emission to space with warming implying a negative cloud anvil feedback on increasing SSTs. The thermostat and iris hypotheses, although based on different mechanisms, both hypothesize that anvil clouds produced by detrainment from deep convection are essentially components of negative feedbacks that buffer the warming of the oceans.

A separate set of hypotheses has been framed around the temperatures of anvil clouds as these clouds rise with the deepening of convection as SSTs warm. In the hypotheses known as fixed anvil temperature (FAT) and proportionately higher anvil temperature (PHAT), anvil cloud temperature remains nearly constant regardless of a surface warming thus resulting in no real change in the OLR as the clouds rise. In this case, the outgoing longwave radiation (OLR) cannot efficiently remove the extra heat associated with the warming (Hartmann and Larson 2002; Zelinka and Hartmann 2010). The clear-sky radiative cooling of the convective environment, however, is fundamental to this idea as the curvature of this cooling in the upper troposphere, in turn defined by the profile of upper tropospheric humidity, defines the heights of convergence required to balance the subsidence driven by the profile of cooling (e.g., Mapes 2001). The feedback involves more than lifting of anvil clouds with deeper convection over warmer SSTs but includes the influence of convection on the environmental upper tropospheric water vapor and the latter, in turn, on radiative cooling which then determines the detrainment level of deep convection. Some aspects of

the FAT feedback are contained in the “stability iris” hypothesis of Bony et al. (2016) who argue, like Lindzen et al. (2001), for a reduction in the detrained anvil cloud cover from convection as SST’s warm effectively producing an IRIS effect but shaped by changes to upper tropospheric stability with warming as opposed to changes in precipitation efficiency of convective storms as proposed by Lindzen et al. (2001).

It is a challenge to use observations to assess the reality of such feedback concepts in any definitive way given the difficulty of assessing the long-term regulation of SSTs with typically short-term observations. Nevertheless, observations must be scrutinized to claim credibility for these feedback ideas. One approach is to test basic understanding of the central processes underlying the hypothesized feedbacks (e.g., Stephens 2005). The results of Figs. 9 and 10 above, for example, offer a test of our understanding of cloud anvil property changes as convection deepens albeit in the context of interannual variability. The observations point to the thickening of anvils associated with deepening convection as most influential on the CREs on those time scales. The study of Ito and Masunaga (2022) is another example of how satellite observations matched to re-analysis data can be used to interrogate hypotheses inherent to feedback concepts. They found that the inter-relationships between anvil cloud fraction, upper tropospheric stability and upper tropospheric convergence are consistent with expectations of the stability iris theory of Bony et al. (2016). By contrast, they further showed that an enhancement in precipitation efficiency is unlikely to have appreciable consequences on the horizontal extent of anvil clouds although admittedly defining the actual precipitation efficiency with observations is challenging and analysis of CMIP6 model data suggest an increased precipitation efficiency with warming with associated reductions in high cloud (e.g., Li et al. 2022).

5.2 Deep Convection, High and Low Clouds and Circulation Driven Feedbacks

Critical to many of the cloud feedback ideas proposed, it is the underlying relation between convection and high clouds detrained from it and how these clouds then modulate the local heating and the circulation that, in turn, affects convection and clouds further afield. Aspects of the topics described above now come together with a discussion framed around Fig. 11a–c. Figure 11a is a schematic summary of the changes in convection, high clouds, OLR, precipitation and far field influences on low clouds via changes to the Hadley circulation that are consequence of the warming expressed as the ECS of climate models. This figure is a conceptual synthesis of 23 model simulations forced by the CMIP6 SSP5-8.5 scenario contrasted against the historical simulations for the period 2000–2014 (e.g., Schiro et al. 2022). The figure is a graphical summary of the discussions of Su et al. (2017) and Schiro et al. (2022) and is a synthesis of model responses for the convective zone between latitudes of 10 N and 10 S (Fig. 11b) and responses in the subtropical regions in latitude ranges 10–20 N/S (Fig. 11c). A prominent feature of the projected tropical circulation change in a warmer climate is the intensification of zonal-mean equatorial ascent flanked by the weakening of upward motion to its north and south resulting in a narrowing of the deep convection zone (e.g., Lau and Kim 2015). This feature is simulated by most climate models and is referred to by Su et al. (2017) as the tightening of Hadley ascent in contrast to the well-known widening of the Hadley cell (e.g., Seidel et al. 2008; Tao et al. 2016). There is an expansion of the surrounding dry regions which are regions that acts as analogous to radiator fins (Pierrehumbert 1995) or are regions described as an expanding iris as proposed by Lindzen et al. (2001) and discussed by Mauritsen and Stevens (2015). This is also a region in which the upper troposphere both dries, the stability increases and

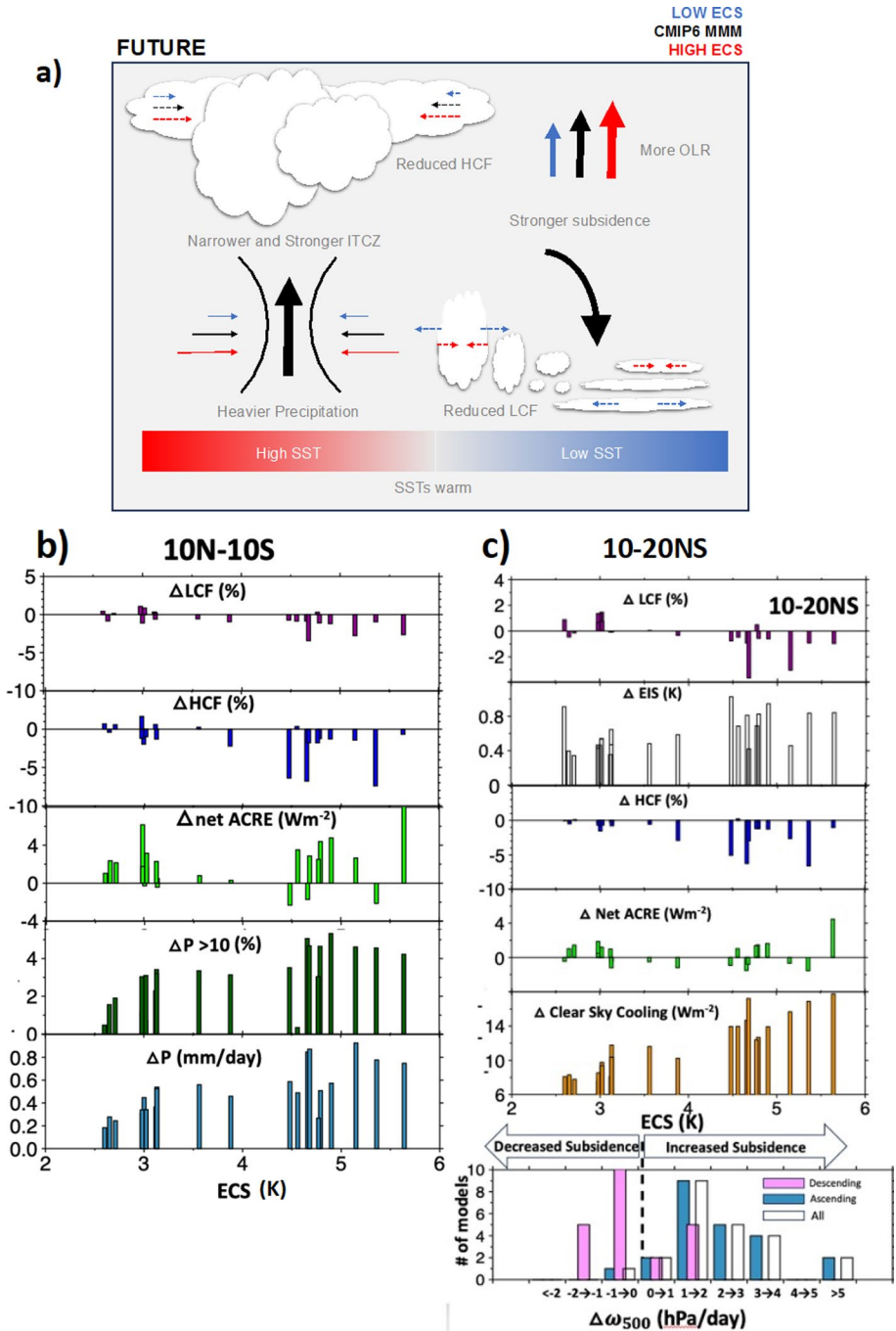


Fig. 11 a A schematic of model simulated changes in the Hadley circulation and tropical clouds along with the OLR and precipitation changes experienced in a warmer climate. The different color arrows signify the degree of warming expressed by the model ECS. The length of the arrows symbolically displays the strength of the process change. **b, c** Specific changes to a number of process defining quantities that reflect on the changes called out in **a** (see text)

high clouds decrease which is a combination consistent with the stability iris hypothesis of Bony et al. (2016). Changes to low clouds that occur in the subtropical regions are linked to the changes that occur in the convective zone.

Study of the model responses conveyed in Fig. 11b and c reveals the following:

- (i) In the 10 N/S latitude convective zone, the precipitation increases both in total amount and in intensity as indicated by the increases in the fraction of precipitation that exceeds 10 mm/day. The ACRE also shows a greater column warming in a manner that might have been anticipated from the analysis of the observational record (e.g., Figure 8). The combination of decreased high cloud cover in this zone of convection and enhanced precipitation, including the more intense precipitation presumably from the deeper convection, is at least broadly consistent with that posited by Lindzen et al. (2001).
- (ii) Most models produce an overall strengthened subsidence in the subtropical regions indicated by positive changes in the 500 hPa vertical velocity (ω_{500}). This enhanced subsidence is consistent with the enhanced clear-sky radiative cooling that results under warming that highly correlates with the ECS ($r=0.93$) and with the increased OLR from the region. The increased radiative cooling is expected given this column cooling proportionally depends on column water vapor (e.g., Stephens et al. 1994). The net changes to vertical motion of the region, however, are realized in a more complex manner than is suggested by bulk changes of the region. The vertical motions in the ascending portions of the region weaken, presumably associated with reduced deep convection in the fringes of the deep convective zone as described above, whereas the vertical motions in the descending regions also weaken as reported by Schiro et al (2022); thus, creating a more complicated response than is conveyed simply in the area-mean vertical motion change (bottom panel of Fig. 11c). Lapse-rate changes that occur result in an increase in the estimated inversion strength (EIS, e.g., Wood and Bretherton 2006) in all models. Although this increase in EIS favors a response of increased low cloud in the subtropical regions (e.g., Klein et al. 2017), the opposite response occurs with most models producing reductions in low clouds.

6 Deep Convection and the Pattern of Warming

The previous sections were concerned with the connections between the large-scale heat transport by the overturning circulations to tropical convection within the tropical region defined as the TTZ. These sections further focus on mechanisms that connect convection in the TTZ to cloudiness and to the radiative responses associated with this cloudiness. This section now expands this view to even larger scales as represented by patterns of change associated with global warming.

It is natural to expect that changes to the overturning circulations induced by a global warming and shaped by the deep convection responses in the tropics would impact and respond to the regional patterns of the warming because of the associated changes in cloud patterns that result. This is a topic now broadly referred to as the “pattern effect” (e.g., Stevens et al. 2016) which encapsulates the finding that the regional details of the patterns of the warming influence the global mean ECS. This influence is expected since climate feedbacks that define the ECS, such as those associated with cloud and lapse-rate changes

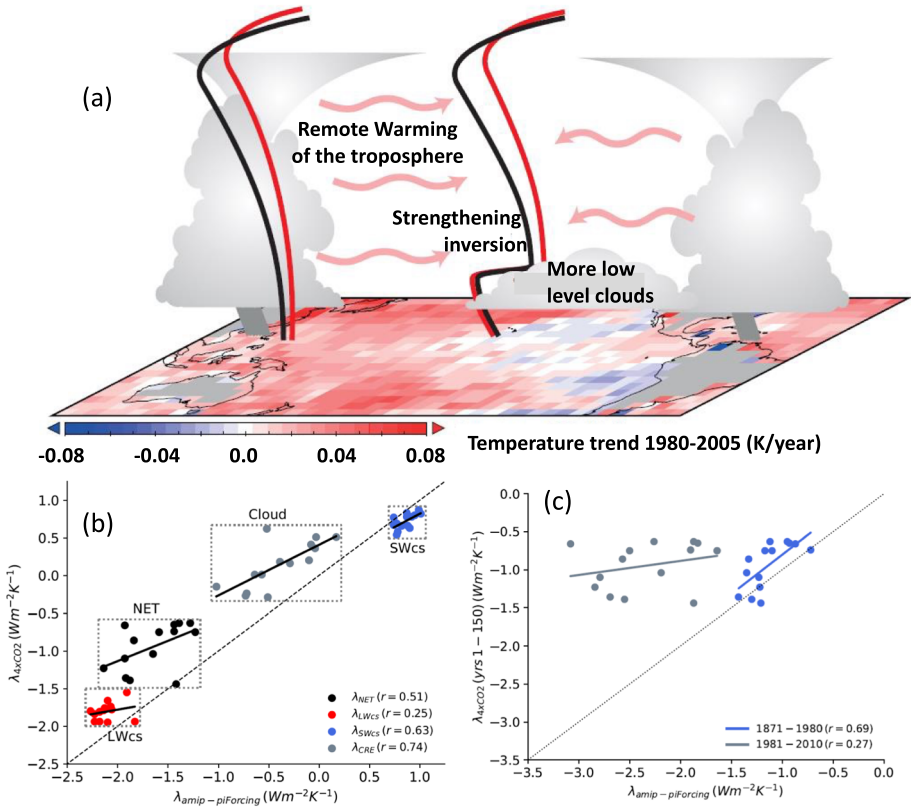


Fig. 12 **a** A schematic of the way warming spreads across the tropical region, **b** relationship across models (dots) between the feedback parameter in amip-piForcing (calculated over years 1871–2010) and abrupt-4xCO₂ simulation (calculated over years 1–150). The net feedback parameter is decomposed into its long-wave clear-sky, shortwave clear-sky and cloud radiative effect components and **c** relationships between model simulated feedbacks in amip-piForcing over years 1871–1980 (blue) or 1981–2010 (gray)—adapted from Mauritsen and Stevens (2015) and Andrews et al. (2022)

(Zhou et al. 2016; Andrews and Webb 2018), vary with the pattern of surface warming. This pattern effect is exemplified in the pattern of warming that occurs across the tropical Pacific Ocean as schematically portrayed in Fig. 12. Warming in the ascent regions of tropical deep convection, particularly in the TWP region, influences the warming throughout the tropical atmosphere. This remote warming gives rise to a potential strong negative lapse rate feedback that results under a scenario of an upper-level warming that extends widely across the tropics that exceeds the surface warming below it. When this occurs, the low cloud controlling factors of EIS, for example, are inductive to increased low cloud amount. This creates a west to east warming-cooling dipole pattern in the tropics that results in a smaller ECS and thus smaller global warming (e.g., Ceppi and Gregory 2017). Under the scenario of the reversed circumstance of stronger surface warming, reduced EIS and reduced low cloud cover, the positive feedback associated with these low cloud reductions drives higher values of ECS and greater warming. We now see how these two contrasting scenarios of patterns effects are found in the historical record of change.

Andrews et al. (2018) quantify the pattern effect using the global “climate feedback parameter” λ as diagnosed from the linearization of the global mean energy budget with global mean surface temperature (e.g., Gregory et al. 2004). They introduce the difference, $\Delta\lambda$, between the feedback deduced from the atmospheric GCM (AGCM) simulation forced by the observed historical SST and sea-ice variations (i.e., the amip-piForcing simulation; λ_{hist}) and the λ inferred from 150 years of a coupled AOGCM abrupt-4xCO₂ simulation with the same AGCM ($\lambda_{4x\text{CO}_2}$) and use $\Delta\lambda = \lambda_{4x\text{CO}_2} - \lambda_{\text{hist}}$ as a measure of this pattern effect. The contributions by clouds on $\Delta\lambda$ can be gleaned in Fig. 12b (after Andrews et al. 2022). The figure is in the form of $\lambda_{4x\text{CO}_2}$ versus λ_{hist} such that deviations from the one-to-one line express the pattern effect. The decomposition of λ into long, shortwave clear-sky contributions and the net radiative effect of clouds clearly illustrates how the bulk of the pattern effect arises from the changing pattern of cloud feedbacks. This analysis reveals net cloud feedbacks that are more negative and less positive in the amip-piForcing experiments than in the abrupt-4xCO₂ experiments.

Figure 12c is presented in the same format as Fig. 12b but now separates the historical responses into two epochs: before and after 1980. The rationale for defining these two epochs, described in more detail in Andrews et al. (2022), is largely revealed in Fig. 12c. The spread in feedback across models over the earlier (1871–1980) time period in amip-piForcing experiments is well correlated with the spread in feedbacks across models in abrupt-4xCO₂ ($r=0.69$). In contrast, feedbacks over the most recent decades (1981–2010) weakly correlate with $\lambda_{4x\text{CO}_2}$ ($r=0.27$) which implies the feedbacks operating in 1871–1980 historical period differ from the feedbacks that govern the responses in 1981–2010. It also implies that inferences about feedbacks in this period do not apply to the feedbacks that establish the longer historical record of change. This is somewhat ironical as it is this latter period that is more intensely observed. It also explains why observational based estimates of ECS from the more recent historical climate change are lower than the ECS inferred from the abrupt experiments: Feedbacks in this more recent period are thought to be more negative in response to observed SST patterns that show a lack of Southern Ocean and Eastern Pacific warming, in contrast to longer term warming seen in paleo and AOGCM data. This further underscores a point called out above—feedbacks that play out on one time scale, such as that suggested from analysis of the current observational period, might not necessarily define the most influential feedbacks associated with longer term, historical climate change.

7 Summary Discussion

This paper revisits the energetics of the tropical trough zone as defined by Riehl and Simpson (1979). A theme of the paper is concerned with how the diabatically-forced overturning circulations of the atmosphere, forced by the deep convection within this tropical zone, fundamentally shape the distributions of tropical and subtropical cloudiness and the changes to cloudiness as Earth warms. The study at first draws on a range of observations to understand the connections between the energetics of the TTZ, convection and clouds. This focus on the TTZ is then expanded with a more global view based on model responses to a forced warming. The main findings of the research described in this paper include:

- (1) The characteristics of convection across the TTZ and the patterns of change over the annual cycle are shown to be more complex than the simple, more classical view of a narrow, quasi-stationary convergence zone typically thought of as the ITCZ such as conveyed in simple depictions like that of Fig. 11. Seasonal changes to precipitation within the TTZ (Fig. 4a) reveal shifting patterns of precipitation, and by inference convection, over the mean annual cycle that is argued to exist as three different regimes within the TTZ. One is the regime of convection over the large southern land masses of S. America and the African continent that follow the movement of the Sun through its annual cycle. A second regime is that of convection confined to narrow convergence zones more typical of the classical view of the ITCZ over the Mid- and Eastern Pacific and tropical Atlantic oceans that are quasi-stationary, locked to the maximum SSTs of these regions. A third regime encapsulates the convection of the maritime continent that by virtue of the complex geography of the region, together with the fact it lies in some of the warmest waters on Earth, creates a complex set of interactions and circulations generated between ocean and land producing complicated precipitation patterns and a broad seasonal cycle tied to the monsoon systems of the region.
- (2) Observations of the two main components of the diabatic heating, the radiative heating as characterized by the ACRE and the latent heating taken to be proportional to the surface precipitation, while additive, reveal a very tight coupling between the two (e.g., Fig. 8) in the TTZ. The reason for such a tight coupling between them and for the magnitude of the slopes of the relationship found in Fig. 8 requires further investigation. This coupling points to a feedback system where one form of heating reinforces the other. Associated far field changes, typically in the form of increased radiative cooling of the surrounding environment, drive thermally direct circulations that also directly influence convection. This has been called out in a number of past studies that argue, for example, that the ACRE can both feedback on convection directly (e.g., Stephens et al. 2004), create a thermally direct circulation that reinforces convection and thus the latent heating (e.g., Wu et al. 2023; Stephens et al. 2008a, 2018), and, in turn, strengthen the larger scale circulation (e.g., Slingo and Slingo 1988; Dixit et al. 2018, among many others). This circulation is also an important mechanism of convective aggregation with further consequences to the TOA energy budget (e.g., Bony et al. 2020).
- (3) Observations of convection, clouds and the energy balance of the TTZ were examined through the perspective of their observed interannual variations over a 20-year period approximately between 2002 and 2022. It was found that:
 - (i) A clear anti-correlation exists between the interannual anomalies of mean tropopause height and the net energy imbalance of the TTZ for a considerable portion of this observed period. The higher the tropopause, the deeper is the convection (Fig. 9). Associated with the deepening of convection is an increase in thickening of anvil clouds with an associated increase of optical depth.
 - (ii) Deeper convection and optically thicker anvils produce an increased reflection of solar radiation that dominates the interannual changes of the net radiation input into the zone (Fig. 10) giving rise to the observed anti-correlation between tropopause height anomalies and TOA radiation budget anomalies.
- (4) One important influence of global warming on the circulation occurs via changes to convection and increased convective heating that strengthen the circulation resulting in a positive low cloud feedback in some models and an enhanced global ECS of these models. Figure 11 provides a summary of the multi-model changes observed under the

scenario of warming realized in the CMIP6 SSP5-8.5 scenario multi-model experiments with the finding that:

- (i) A pronounced narrowing of the ITCZ occurs with an associated increase in precipitation including increased heavy precipitation. Such a projected narrowing of the ITCZ is also supported in precipitation observations from 1979 to 2014 (Wodzicki and Rapp 2019). Whether contraction of convection such as observed in the Eastern Pacific applies to convection formed over the maritime continent or over tropical land masses is yet to be studied although the related study of Roca et al. (2024) finds that convection over Africa has changed in its morphology over four decades of Meteosat observations with a significant shift of the occurrence of deep convective systems to less frequent large and short-lived systems to more frequent smaller and longer-lived systems. Twentieth century observations also show that, during the last 50 years, the sea surface temperature (SST) of the tropical oceans has increased by 0.5C and the areas of SST > 26.5 and 28C by 15 and 50%, respectively, in association with an increase in greenhouse gas concentrations (Hoyas and Webster 2012). We do not know how convection responds to this expanded area of warmed SSTs and whether there will be any contraction of convection in this zone.
- (ii) Although precipitation increases in the tropical convective zone in models, the high clouds do not (Fig. 11b) but the column radiative heating does via reduction on low cloud that act as net coolers of the column. In the subtropical regions, the clear-sky radiative cooling increases as expected from increased water vapor, thus setting up a differential heating patterns consistent with a strengthening of the meridional circulation as speculated in a number of studies (e.g., Needham and Randall 2021a, 2021b; Stephens et al 2018; Dixit et al. 2018) and consistent with the projected increased subsidence (Fig. 11c).
- (iii) The multi-model response of a combined reduction in high clouds and increased precipitation in the convection zone is also consistent with the Lindzen et al. (2001) iris mechanism that the precipitation efficiency of convection should increase with warming with proportionally more water falling out as precipitation than is vertically advected and detained aloft. This still remains an unproven concept (e.g., Ito and Masunaga 2022) although other model studies support it (e.g., Li et al. 2022).
- (iv) In the subtropical regions (Fig. 11c), most models produce a strengthened subsidence, constrained overall by clear-sky radiative cooling increases but how this increased subsidence is realized is complicated with reduced vertical motion in both ascending and descending regions of the subtropics. Lapse rate changes also result in an increase in the EIS. While this increase in EIS favors increased low cloud responses in the subtropical regions, most models, and notably those with highest ECS, experience reduced low clouds in this region which appears to be an important feedback mechanism that sustains the higher ECS (e.g., Schiro et al. 2022). These model low cloud changes involve more than changes to simple cloud controlling factors like EIS, at least in the CMIP6 SSP5-8.5 scenario experiments (e.g., Koshiro et al. 2022).
- (5) Specific details of the pattern of warming influence the global mean response of models: This influence, referred to as the pattern effect, is exemplified in the pattern of warming across the tropical Pacific Ocean which is influenced by the low cloud responses on the Eastern Pacific SSTs. Andrews et al. (2022) quantify this effect as a difference between the feedback metrics derived as the difference in the feedback measures of the CMIP6 amip-piForcing experiments from the CMIP6 abrupt-4xCO₂, the rationale being that feedbacks calculated from 150 years of the abrupt experiments that strongly correlate to longer term projections of climate change will have a weaker pattern effect

than when the correlation is much weaker. They found that over the period 1871–1980, the Earth warmed with feedbacks largely consistent and strongly correlated with long-term climate sensitivity feedbacks—that is the historical pattern of warming mirrors that change expected of the future (as diagnosed from corresponding atmosphere–ocean GCM abrupt-4xCO₂ simulations). Post 1980, however, the Earth warmed with patterns of warming that differ from past historical warming being weakly correlated to feedbacks of the abrupt experiments (Fig. 12). The basic conclusion is the feedbacks operating in 1871–1980 historical period differs from the feedbacks that govern the responses in 1981–2010. This is somewhat ironical as it is this latter period that is more intensely observed and processes that undergird feedbacks are better understood. Andrews et al. (2022) further reason that it also explains why observational based estimates of ECS from the more recent historical climate change are likely biased low.

The science of climate change and the study of feedbacks that define the overall climate sensitivity appear to face a fundamental dilemma. There are a number of examples presented throughout this paper where mechanisms observed over shorter time spans may not be the dominant mechanisms of feedbacks that play out on longer time scales. For example, the thickening and brightening of anvil clouds described above and observed on interannual time scales are not reflected in the high cloud responses of climate models as described in Sect. 5. A second example was illustrated in the study of Andrews et al. (2022), where the more recent, shorter period observational record points to mechanisms and feedbacks involving cloud and convection that apparently do not define the feedbacks that establish longer term projected changes diagnosed from models. One could argue that the processes examined during the more recent intensely observed period are intrinsically those that must operate over the longer period of change albeit with different degrees of interaction. How can the credibility of projections be claimed while dismissing the observed natural state and its behaviors of the shorter past? What then is the role of observing the natural world and studying how processes interact from that vantage point if these are not deemed relevant to a longer term climate change? What then are the relevant observations that are unequivocal tests of feedbacks most pertinent to climate change for without them model projections will remain purely untested hypotheses? Regardless of these challenges, the need to quantify the role of deep convection in the Earth system remains acute.

The coming decade is also a decade that brings a focus on atmospheric convection. The desire to resolve convection is now a major focus of next generation Earth models (e.g., Slingo et al. 2022). From an observational perspective, major inroads to observing convection on the global scale are also about to happen. These observational programs are meant to address a high priority needs as called out in the 2017 Decadal Survey (NAS 2018). Two important new measurement initiatives of the current decade that address convection specifically are: i) the INvestigation of Convective UpdraftS (INCUS) mission of NASA that is to provide basic global information about convective motions and the transports produced by them, and ii) NASA's Earth System Observatory (the Atmospheric Observing System (AOS) <https://aos.gsfc.nasa.gov>),¹ aimed at addressing the Decadal priority by providing information about convective updraft and downdraft motions with space-borne Doppler radars. AOS will also include the tandem microwave radiometer measurements aimed at further quantifying vertical transports in deep convection (e.g., Brogneiz et al. 2022).

¹ The decadal strategy identified observations of aerosol, cloud, convection and precipitation as a priority for the decade. This priority has led to the definition of NASA's atmospheric observing system (AOS).

Acknowledgements This paper is an outcome of the Workshop "Challenges in Understanding the Global Water Energy Cycle and its Changes in Response to Greenhouse Gas Emissions" held at the International Space Science Institute (ISSI) in Bern, Switzerland (26–30 September 2022). © 2024. All rights reserved. Government sponsorship acknowledged.

Funding The lead author was supported in part by INCUS, Libera and by CloudSat, each being NASA Earth Venture Missions, funded by NASA's Science Mission Directorate and managed through the Earth System Science Pathfinder Program. Portions of the research described in this paper were performed at the Jet Propulsion Laboratory, California Institute of Technology under contract with the National Aeronautics and Space Administration. T.A. was supported by the UK Meteorological Office Hadley Centre Climate Program funded by the Department of Business, Energy and Industrial Strategy and received funding from the European Union's Horizon 2020 research and innovation program under Grant Agreement 820829. K.A.S. is supported by the National Science Foundation Grant # 2225954.

Data availability The radiative heating rate data will be available via <https://gewex-utcc-proes.aeris-data.fr/>.

Declarations

Conflict of Interest The authors declare no conflicts of interest.

Open Access This article is licensed under a Creative Commons Attribution 4.0 International License, which permits use, sharing, adaptation, distribution and reproduction in any medium or format, as long as you give appropriate credit to the original author(s) and the source, provide a link to the Creative Commons licence, and indicate if changes were made. The images or other third party material in this article are included in the article's Creative Commons licence, unless indicated otherwise in a credit line to the material. If material is not included in the article's Creative Commons licence and your intended use is not permitted by statutory regulation or exceeds the permitted use, you will need to obtain permission directly from the copyright holder. To view a copy of this licence, visit <http://creativecommons.org/licenses/by/4.0/>.

References

- Andrews T, Webb MJ (2018) The dependence of global cloud and lapse rate feedbacks on the spatial structure of tropical Pacific warming. *J Climate* 31(2):641–654. <https://doi.org/10.1175/JCLI-D-17-0087.1>
- Andrews T, Gregory JM, Paynter D, Silvers LG, Zhou C, Mauritsen T et al (2018) Accounting for changing temperature patterns increases historical estimates of climate sensitivity. *Geophys Res Lett* 45(16):8490–8499. <https://doi.org/10.1029/2018GL078887>
- Andrews T, Bodas-Salcedo A, Gregory JM, Dong Y, Armour KC, Paynter D et al (2022) On the effect of historical SST patterns on radiative feedback. *J Geophys Res: Atmos* 127:e2022JD036675. <https://doi.org/10.1029/2022JD036675>
- Bony S et al (2016) Thermodynamic control of anvil cloud amount. *Proc Natl Acad Sci* 113:8927–8932
- Bony S, Semie A, Kramer RJ, Soden B, Tompkins AM, Emanuel KA (2020) Observed modulation of the tropical radiation budget by deep convective organization and lower-tropospheric stability. *AguAdvances* 1:e2019AV00155. <https://doi.org/10.1029/2019AV000155>
- Boucher O, Randall D, Artaxo P, Bretherton C, Feingold G, Forster P, Kerminen V-M, Kondo Y, Liao H, Lohmann U, Rasch P, Satheesh SK, Sherwood S, Stevens B, Zhang XY (2013) Clouds and aerosols. In: Stocker TF, Qin D, Plattner G-K, Tignor M, Allen SK, Boschung J, Nauels A, Xia Y, Bex V, Midgley PM (eds) *Climate change 2013: the physical science basis. contribution of working group I to the 5th assessment report of the intergovernmental panel on climate change*. Cambridge University Press, Cambridge, New York
- Broccoli AJ, Dahl KA, Stouffer RJ (2006) Response of the ITCZ to Northern Hemisphere cooling. *Geophys Res Lett* 33:01702. <https://doi.org/10.1029/2005GL024546>
- Brognez H, Roca R, Auguste F, Chaboureaud J-P, Haddad Z, Munchak SJ, Li X, Bouniol D, Dépée A, Fiolleau T, Kollias P (2022) Time-delayed tandem microwave observations of tropical deep convection: overview of the C2OMODO mission. *Front Remote Sens* 3:854735. <https://doi.org/10.3389/frsen.2022.854735>


- Ceppi P, Gregory JM (2017) Relationship of tropospheric stability to climate sensitivity and Earth's observed radiation budget. *Proc Natl Acad Sci USA* 114(50):13126–13131. <https://doi.org/10.1073/pnas.1714308114>
- Crespo LR, Keenlyside N, Koseki S (2019) The role of sea surface temperature in the atmospheric seasonal cycle of the equatorial Atlantic. *Clim Dyn* 52:5927–5946. <https://doi.org/10.1007/s00382-018-4489-4>
- Davis SM, Liang CK, Rosenlof KH (2013) Interannual variability of tropical tropopause layer clouds. *Geophys Res Lett* 40(11):2862–2866
- Dee DP et al (2011) The ERA-Interim reanalysis: configuration and performance of the data assimilation system. *Q J R Meteorol Soc* 137:553–597. <https://doi.org/10.1002/qj.828>
- Derras-Chouk A, Luo ZJ (2024) Revisiting Riehl and Malkus (1958) and Riehl and Simpson (1979): characterizing tropical hot towers and estimating convective mass fluxes using geostationary satellite data. *Surv Geophys (ISSI special issue)* (to submitted)
- Dessler AE (2010) A determination of the cloud feedback from climate variations over the past decade. *Science* 330:1523–1527. <https://doi.org/10.1126/science.1192546>
- Dixit V, Geoffroy O, Sherwood SC (2018) Control of ITCZ width by low-level radiative heating from upper-level clouds in aqua-planet simulations. *Geophys Res Lett* 45:5788–5797. <https://doi.org/10.1029/2018GL078292>
- Eyring V, Bony S, Meehl GA, Senior CA, Stevens B, Stouffer RJ, Taylor KE (2016) Overview of the coupled model intercomparison project phase 6 (CMIP6) experimental design and organization. *Geosci Model Dev* 9:1937–1958. <https://doi.org/10.5194/gmd-9-1937-2016>
- Forget G, Campin J-M, Heimbach P, Hill CN, Ponte RM, Wunsch C (2015) ECCO version 4: an integrated framework for non-linear inverse modeling and global ocean state estimation. *Geosci Model Dev*. <https://www.geosci-model-dev.net/8/3071/2015/>
- Frierson DM, Hwang YT (2012) Extratropical influence on ITCZ shifts in slab ocean simulations of global warming. *J Clim* 25(2):720–733
- Fueglistaler S, Dessler AE, Dunkerton TJ, Folkins I, Fu Q, Mote PW (2009) Tropical tropopause layer. *Rev Geophys* 47:1004. <https://doi.org/10.1029/2008RG000267>
- Gray WM, Jacobsen Jr RW (1977) Diurnal variation of deep cumulus convection. *Mon Wea Rev* 105:1171–1188. [https://doi.org/10.1175/1520-0493\(1977\)105<1171:DVOGCC>2.0.CO;2](https://doi.org/10.1175/1520-0493(1977)105<1171:DVOGCC>2.0.CO;2)
- Gregory JM, Ingram WJ, Palmer MA, Jones GS, Stott PA, Thorpe RB et al (2004) A new method for diagnosing radiative forcing and climate sensitivity. *Geophys Res Lett* 31(3):L03205. <https://doi.org/10.1029/2003GL018747>
- Guzman R, Chepfer H, Noel V, Vaillant de Guélis T, Kay JE, Raberanto P, Cesana P, Vaughan MA, Winker DM (2017) Direct atmosphere opacity observations from CALIPSO provide new constraints on cloud-radiation interactions. *J Geophys Res Atmos* 122:1066–1085. <https://doi.org/10.1002/2016JD025946>
- Harrop BE, Hartmann DL (2016) The role of cloud radiative heating in determining the location of the ITCZ in aqua-planet simulations. *J Climate* 29(8):2741–2763
- Hartmann DL, Larson K (2002) An important constraint on tropical cloud-climate feedback. *Geophys Res Lett* 29(20):1951–1954
- Hoyos CD, Webster PJ (2012) Evolution and modulation of tropical heating from the last glacial maximum through the twenty-first century. *Clim Dyn* 38:1501–1519. <https://doi.org/10.1007/s00382-011-1181-3>
- Huffman GJ, Bolvin DT, Braithwaite D, Hsu KL, Joyce RJ, Kidd C, Nelkin EJ, Sorooshian S, Stocker EF, Tan J, Wolff DB (2020) Integrated multi-satellite retrievals for the global precipitation measurement (GPM) mission (IMERG). In: Levizzani V, Kidd C, Kirschbaum D, Kummerow C, Nakamura K, Turk F (eds) *Satellite precipitation measurement. Advances in global change research*, vol 67, pp 343–353. https://doi.org/10.1007/978-3-030-24568-9_19
- Ito M, Masunaga H (2022) Process level assessment of the iris effect over tropical oceans. *Geophys Res Lett* 49:e2022GL097997. <https://doi.org/10.1029/2022GL097997>
- Kang SM, Held IM, Frierson DM, Zhao M (2008) The response of the ITCZ to extratropical thermal forcing: idealized slab-ocean experiments with a GCM. *J Clim* 21(14):3521–3532
- Kang SM, Frierson DM, Held IM (2009) The tropical response to extratropical thermal forcing in an idealized GCM: The importance of radiative feedbacks and convective parameterization. *J Atmos Sci* 66(9):2812–2827
- Kato S et al (2018) Surface irradiances of edition 4.0 clouds and the earth's radiant energy system (CERES) energy balanced and filled (EBAF) data product. *J Climate* 31:4501–4527
- Kiehl JT (1994) On the observed near cancellation between longwave and shortwave cloud forcing in tropical regions. *J Climate* 7:559–565
- Klein SA, Hall A, Norris JR, Pincus R (2017) Low-cloud feedbacks from cloud-controlling factors: a review. *Surv Geophys* 38:1307–1329. <https://doi.org/10.1007/s10712-017-9433-3>

- Knutti R, Rugenstein M, Hegerl G (2017) Beyond equilibrium climate sensitivity. *Nature Geosci* 10:727–736. <https://doi.org/10.1038/ngeo3017>
- Koshiro T, Kawai H, Noda AT (2022) Estimated cloud-top entrainment index explains positive low-cloud-cover feedback. *PNAS* 119:e2200635119. <https://doi.org/10.1073/pnas.2200635119>
- Lau WK, Kim KM (2015) Robust Hadley circulation changes and increasing global dryness due to CO2 warming from CMIP5 model projections. *Proc Natl Acad Sci* 112:3630–3635
- Li Y, Thompson DW (2013) The signature of the stratospheric Brewer–Dobson circulation in tropospheric clouds. *J Geophys Res Atmos* 118(9):3486–3494
- Li Y, Thompson DW, Bony S (2015) The influence of atmospheric cloud radiative effects on the large-scale atmospheric circulation. *J Clim* 28(18):7263–7278
- Li RL, Studholme JH, Fedorov AV, Storelvmo T (2022) Precipitation efficiency constraint on climate change. *Nat Clim Chang* 12(7):642–648
- Lindzen RS, Chou M-D, Hou AY (2001) Does the Earth have an adaptive infrared iris? *Bull Am Meteorol Soc* 82(3):417–432. <https://doi.org/10.1175/1520-0477>
- Loeb NG et al (2018) Clouds and the Earth’s radiant energy system (CERES) energy balanced and filled (EBAF) top-of-atmosphere (TOA) edition 4.0 data product. *J Clim*. <https://doi.org/10.1175/jcli-d-17-0208.1>
- Luo Z, Liu GY, Stephens GL (2008) CloudSat adding new insight into tropical penetrating convection. *Geophys Res Lett* 35:L19819. <https://doi.org/10.1029/2008GL035330>
- Mace GG, Zhang Q, Vaughan M, Marchand R, Stephens G, Trepte C, Winker D (2009) A description of hydrometeor layer occurrence statistics derived from the first year of merged cloudsat and CALIPSO data. *J Geophys Res*. <https://doi.org/10.1029/2007JD009755>
- Machado LAT, Rossow WB (1993) Structural characteristics and radiative properties of tropical cloud clusters. *Mon Wea Rev* 121:3234–3260
- Mapes BE (2001) Water Vapor two scale heights: the moist adiabat and the radiative troposphere. *Q J R Meteorol Soc* 127:2353–2366
- Mauritsen B, Stevens B (2015) Missing iris effect as a possible cause of muted hydrological change and high climate sensitivity in models. *Nat Geosci* 8(5):346–351. <https://doi.org/10.1038/ngeo2414>
- National Academies of Sciences, Engineering, and Medicine (2018) Thriving on our changing planet: a decadal strategy for earth observations from space. The National Academies Press, Washing. <https://doi.org/10.17226/24938>
- Needham MR, Randall DA (2021a) Linking atmospheric cloud radiative effects and tropical precipitation. *Geophys Res Lett* 48:e2021GL094004. <https://doi.org/10.1029/2021GL094004>
- Needham MR, Randall DA (2021b) Riehl and Malkus revisited: the role of cloud-radiative effects. <https://doi.org/10.1002/essoar.10506726.1>
- Philander SGH, Gu D, Lambert G, Li T, Halpern D, Lau NC, Pacanowski RC (1996) Why the ITCZ is mostly north of the equator. *J Clim* 9(12):2958–2972
- Pierrehumbert RT (1995) Thermostats, radiator fins, and the local runaway greenhouse. *J Atmos Sci* 52:1784–1806
- Pilewskie J, Stephens G, L’Ecuyer T, Takahashi H (2024) A multi-satellite perspective on “hot tower” characteristics in the equatorial trough zone, *Surv Geophys*
- Popp M, Silvers LG (2017) Double and single ITCZs with and without clouds. *J Clim* 30(22):9147–9166
- Ramanathan V, Collins W (1991) Thermodynamic regulation of ocean warming by cirrus clouds deduced from observations of the 1987 El Niño. *Nature* 351:27–32
- Riehl H, (Malkus) Simpson J (1979) The heat balance of the equatorial trough zone, revisited. *Contr Atmos Phys* 52:287–305
- Riehl H, Malkus JS (1958) On the heat balance in the equatorial trough zone. *Geophysica* 6:503–537
- Roca R, Fiolleau T, John VO, Schulz J (2024) METEOSAT long term observations reveal changes in convective organization over tropical Africa and Atlantic Ocean. *Surv Geophys*
- Schiro KA, Su H, Ahmed F et al (2022) Model spread in tropical low cloud feedback tied to overturning circulation response to warming. *Nat Commun* 13:7119. <https://doi.org/10.1038/s41467-022-34787-4>
- Seidel DJ, Fu Q, Randel WJ, Reichler TJ (2008) Widening of the tropical belt in a changing climate. *Nat Geosci* 1:21–24
- Sherwood SC, Ramanathan V, Barnett TP, Tyree MK, Roeckner E (1994) Response of an atmospheric general circulation model to radiative forcing of tropical clouds. *J Geophys Res* 99(D10):20829–20845
- Slingo JM, Bates P, Belcher S, Palmer T, Stephens G, Stevens B (2022) Ambitious partnership needed for reliable climate prediction. *Nat Clim Chang*. <https://doi.org/10.1038/s41558-022-01384-8>
- Slingo A, Slingo JM (1988) The response of a general circulation model to cloud longwave radiative forcing. I: introduction and initial experiments. *Q J R Meteorol Soc* 114(482):1027–1062. <https://doi.org/10.1002/qj.49711448209>

- Sokol AB, Hartmann DL (2020) Tropical anvil clouds: Radiative driving toward a preferred state. *J Geophys Res Atmos* 125:e2020JD033107. <https://doi.org/10.1029/2020JD033107>
- Stephens GL (2005) Cloud feedbacks in the climate system: a critical review. *J Clim* 18:237–273
- Stephens GL, Webster PJ, Johnson RH, Engelen R, L'Ecuyer TS (2004) Observational evidence for the mutual regulation of the tropical hydrological cycle and tropical sea surface temperatures. *J Climate* 17:2213–2224
- Stephens GL, van den Heever S, Pakula LA (2008) Radiative convective feedback in idealized states of radiative-convective equilibrium. *J Atmos Sci* 65:3899–3916
- Stephens GL, Hakuba MZ, Webb MJ, Lebsack M, Yue Q, Kahn BH et al (2018) Regional intensification of the tropical hydrological cycle during ENSO. *Geophys Res Lett* 45:4361–4370. <https://doi.org/10.1029/2018GL077598>
- Stephens GL, Hu Y (2010) Are climate-related changes to the character of global precipitation predictable? *Environ Res Lett*. <https://doi.org/10.1088/1748-9326/5/2/025209>
- Stephens GL, Slingo A, Webb MJ, Minnett PJ, Daum PH, Kleinman L, Wittmeyer I, Randall DA (1994) Observations of the earth's radiation budget in relation to atmospheric hydrology 4. Atmospheric column radiative cooling over the world's oceans. *J Geophys Res* 99(D9):18585–18604
- Stephens GL et al (2008) CloudSat mission: performance and early science after the first year of operation. *J Geophys Res* 113:D00A18. <https://doi.org/10.1029/2008JD009982>
- Stevens B, Sherwood SC, Bony S, Webb MJ (2016) Prospects for narrowing bounds on Earth's equilibrium climate sensitivity. *Earth's Fut* 4(11):512–522. <https://doi.org/10.1002/2016EF000376>
- Stubenrauch CJ, Caria G, Protopapadaki SE, Hemmer F (2021) 3D radiative heating of tropical upper tropospheric cloud systems derived from synergistic A-Train observations and machine learning. *Atmos Chem Phys* 21:1015–1034. <https://doi.org/10.5194/acp-21-1015-2021>
- Su H et al (2017) Tightening of tropical ascent and high clouds key to precipitation change in a warmer climate. *Nat Commun* 8:1–9
- Takahashi H, Luo ZJ (2012) Where is the level of neutral buoyancy for deep convection? *Geophys Res Lett* 39:L15809. <https://doi.org/10.1029/2012GL052638>
- Takahashi H, Luo ZJ (2014) Characterizing tropical overshooting deep convection from joint analysis of CloudSat and geostationary satellite observations. *J Geophys Res Atmos* 119:112–121. <https://doi.org/10.1002/2013JD020972>
- Takahashi H, Luo ZJ, Stephens GL (2017) Level of neutral buoyancy, deep convective outflow, and convective core: new perspectives based on 5 years of CloudSat data. *J Geophys Res Atmos* 122:2958–2969. <https://doi.org/10.1002/2016JD025969>
- Takahashi H, Luo ZJ, Stephens G, Mulholland JP (2023) Revisiting the land-ocean contrasts in deep convective cloud intensity using global satellite observations. *Geophys Res Lett* 50:e2022GL102089
- Tao L, Hu Y, Liu J (2016) Anthropogenic forcing on the Hadley circulation in CMIP5 simulations. *Clim Dyn* 46:3337–3350
- Webster P (1994) The role of hydrological processes in ocean-atmosphere interaction. *Rev of Geophys* 32:427–476
- Wei Y, Pu Z, Zhang C (2020) Diurnal cycle of precipitation over the maritime continent under modulation of MJO: perspectives from cloud-permitting scale simulations. *J Geophys Res Atmos* 125:e2020JD032529. <https://doi.org/10.1029/2020JD032529>
- Wodzicki KR, Rapp AD (2019) Long-term characterization of the Pacific ITCZ using TRMM, GPCP, and ERA-Interim. *J Geophys Res Atmos* 121:3153–3170
- Wood R, Bretherton CS (2006) On the relationship between stratiform low cloud cover and lower-tropospheric stability. *J Clim* 19(24):6425–6432
- Wu S-N, Soden BJ, Alaka, Jr GJ (2023) The influence of radiation on the prediction of tropical cyclone intensification in a forecast model. *Geophys Res Lett* 50:e2022GL099442. <https://doi.org/10.1029/2022GL099442>
- Zelinka MD, Hartmann DL (2010) Why is longwave cloud feedback positive? *J Geophys Res Atmos* 115:D16–D117
- Zhou C, Zelinka MD, Klein SA (2016) Impact of decadal cloud variations on the Earth's energy budget. *Nat Geosci* 9(12):871–875. <https://doi.org/10.1038/ngeo2828>
- Zipser EJ, Cecil DJ, Liu C, Nesbitt SW, Yorty DP (2006) Where are the most intense thunderstorms on Earth? *Bull Am Meteorol Soc*. <https://doi.org/10.1175/BAMS-87-8-1057>

Publisher's Note Springer Nature remains neutral with regard to jurisdictional claims in published maps and institutional affiliations.

Authors and Affiliations

Graeme L. Stephens^{1,2}  · **Kathleen A. Shiro**³ · **Maria Z. Hakuba**¹ · **Hanii Takahashi**¹ · **Juliet A. Pilewskie**⁴ · **Timothy Andrews**⁵ · **Claudia J. Stubenrauch**^{6,7} · **Longtao Wu**¹

✉ Graeme L. Stephens
graeme.stephens@jpl.nasa.gov

¹ Jet Propulsion Laboratory, California Institute of Technology, Pasadena, CA 91011, USA

² Department of Physics, University of Oxford, Oxford, OX1 3PJ, UK

³ Department of Environmental Sciences, University of Virginia, Charlottesville, VA 22904-4123, USA

⁴ Department of Atmospheric and Oceanic Sciences, University of Wisconsin-Madison, Madison, WI 53706, USA

⁵ Met Office Hadley Centre, Exeter EX1 3PB, UK

⁶ Laboratoire de Météorologie Dynamique/Institute Pierre-Simon Laplace, (LMD/IPSL), CNRS, Sorbonne Universities, University Pierre and Marie Curie (UPMC) Paris, University of Paris, Paris Cedex 5, Paris 75252, France

⁷ Laboratoire de Météorologie Dynamique/Institute Pierre-Simon Laplace, (LMD/IPSL), CNRS, Ecole Polytechnique, Université Paris-Saclay, 91128 Palaiseau, France